

Kinetic Study of Catalytic Hydrogenation of Thiophene on a Palladium Sulfide Catalyst

A. Ermakova, A. V. Mashkina, and L. G. Sakhaltueva

Boreskov Institute of Catalysis, Siberian Division, Russian Academy of Sciences, Novosibirsk, 630090 Russia

Received July 12, 2001

Abstract—The kinetics of thiophene hydrogenation on a palladium sulfide catalyst is studied at high hydrogen pressures. The reaction mainly occurs via the consecutive scheme: the reaction of thiophene with hydrogen results in the formation of tetrahydrothiophene, which partially decomposes under the action of hydrogen to yield butane and hydrogen sulfide. A kinetic model describing the reaction rates and the selectivity to tetrahydrothiophene at 0.2–3.0 MPa and 493–533 K is proposed. The rate constants and activation energies are determined. The effect of temperature and pressure on the maximal yield of tetrahydrothiophene is examined.

INTRODUCTION

Tetrahydrothiophene is used both as a gas odorant and as a starting material for synthesizing physiologically active substances, polymers, and extracting agents. A promising method for tetrahydrothiophene synthesis is the catalytic thiophene hydrogenation [1]. In the presence of cobalt (nickel)–molybdenum (tungsten) catalysts of hydrorefining, thiophene hydrogenolysis dominates, whereas tetrahydrothiophene is formed in a small yield [2]. The use of palladium sulfide catalysts increases the selectivity to tetrahydrothiophene [3]. The kinetics of the gas-phase hydrogenation of thiophene in the presence of these catalysts has not been studied, and thus the determination of the optimal conditions for this reaction cannot be determined.

In this work, we studied the kinetics of thiophene hydrogenation in the presence of the IK-73-4 palladium sulfide catalyst.

EXPERIMENTAL

Thiophene and tetrahydrothiophene were reagent grade. The experiments were carried out in a flow reactor with a fixed catalyst bed. The setup consisted of a catalytic unit, including a reactor (height, 200 mm; inner diameter, 12 mm), a time-lag-free furnace, six-way valves placed in an oven, a system of gaseous reagent supply (including a thermostatted saturator and cylinders with hydrogen, helium, and a hydrogen sulfide–hydrogen mixture), and an analyzer (a chromatograph connected to a reactor). After passing through a pressure gauge and a saturator with thiophene, hydrogen from a cylinder entered the reactor heated with the

time-lag-free furnace. Upon attaining a stationary regime, the gas composition at the reactor outlet was analyzed with a Tsvet-500 chromatograph with a thermal conductivity detector (a 2 m × 3 mm column filled with Porapak Q+R (1 : 1); gas carrier, helium).

All the experiments were carried out in the absence of the diffusion control using a catalyst sample with a particle size of 0.25–0.5 mm. A decrease in the grain size to 0.1–0.16 mm had no effect on the reaction rate. A freshly activated catalyst sample was used in each run. Gas consumption in the experiments was varied from 20 to 200 mmol/h, the catalyst loading (*m*, kg) was 0.02–0.2 g, and the total pressure was varied within 0.2–3 MPa at 493–533 K. The thiophene concentration in the entering gas flow was 0.9–1.2 mol %.

RESULTS AND DISCUSSION

Influence of the Contact Time on the Reaction Mixture Composition

Table 1 presents the primary data obtained at 2.06 MPa and 493, 513, and 533 K. As in [4, 5], we express the contact time τ as a ratio of the catalyst weight to the overall molar flow of the mixture at the reactor inlet (g s mmol^{-1}) and the concentrations (in mol %) as $100y_i$, where y_i represents the molar fractions. The molar fraction of hydrogen y_{H_2} (not given in the tables) is $y_{\text{H}_2} = 1 - \sum y_i$. Table 1 presents the relative errors in the carbon and sulfur balance calculated as follows

$$\Delta[\text{C}] = ([\text{C}]_{\text{in}} - [\text{C}]_{\text{out}})100/[\text{C}]_{\text{in}},$$

$$\Delta[\text{S}] = ([\text{S}]_{\text{in}} - [\text{S}]_{\text{out}})100/[\text{S}]_{\text{in}},$$

where $[C]_{in}$, $[C]_{out}$, $[S]_{in}$, and $[S]_{out}$ are the flows at the inlet and outlet of the reactor, g-atom/s). The equality $\Delta[S] = \Delta[C]$ follows directly from the balance equations of chemical elements and the stoichiometry of chemical reactions. The balance with respect to hydrogen is fulfilled accurate to 0.5–1% (these data are not given in the tables). Averaged over all the runs, the experimental error was 15–20% for tetrahydrothiophene and 10% for thiophene and hydrogen sulfide.

Table 1 shows that the tetrahydrothiophene concentration passes through a maximum as the contact time increases. Therefore, two main stoichiometric reactions can occur in the system: thiophene hydrogenation to tetrahydrothiophene



and tetrahydrothiophene hydrogenolysis with hydrogen sulfide and butane liberation



Reactions (I) and (II) occur with a decrease in the number of moles. Taking into account a great hydrogen excess in the reaction mixture, the value of γ , expressed as $\gamma \equiv N(\tau)/N^0$, changes a little and insignificantly deviates from unity. Here, $N(\tau)$ and N^0 stand for the molar flows at the reactor outlet and inlet, respectively. We set the γ value equal to unity in further calculations.

Reaction Rate Equations

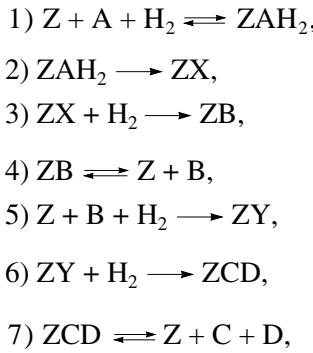
The surface of the palladium sulfide catalyst contains surface acid sites (Z), which form a thiophenium cation when they interact with thiophene (A) [6]. The addition of one hydrogen molecule to this cation results in the formation of an intermediate ZAH_2 , whose further transformation yields dihydrothiophene ZX, which is then hydrogenated to tetrahydrothiophene ZB. The latter desorbs and converts into B and leaves Z-sites unoccupied. The catalytic reaction of thiophene with hydrogen via dihydrothiophene formation was hypothesized in [7, 8]. Temkin *et al.* [9] and van Meerten and Coenen [10] suggested that the hydrogenation of benzene and its derivatives, related to thiophene, involves the stage of formation of a dehydrogenated compound and that the hydrogenation of the latter, which is not aromatic, occurs more rapidly than its formation. The resulting tetrahydrothiophene and hydrogen bind to the site Z to give a surface complex (ZY) containing one hydrogen molecule and tetrahydrothiophene with one obviously broken C–S bond. The intermediate compound ZY rapidly reacts with the second hydrogen molecule to give surface-bound butane (C) and hydrogen sulfide (D) [8], which desorb and leave the Z sites unoccupied.

The formal mechanism of thiophene hydrogenation into tetrahydrothiophene and tetrahydrothiophene

Table 1. Influence of the contact time ($P = 2.06$ MPa, $m_{Cat} = 0.2$ g) on the reaction mixture composition (mol %)

τ , g s mmol ⁻¹	Thio- phene	Tetrahy- drothiophene	H ₂ S	C ₄ H ₁₀	$\Delta[S] = \Delta[C], \%$
<i>T</i> = 493 K					
0.000	1.095	0.000	0.000	0.000	–
8.089	0.695	0.262	0.040	0.040	8.95
11.430	0.624	0.411	0.078	0.078	–1.64
12.200	0.500	0.384	0.077	0.077	12.24
14.400	0.460	0.448	0.202	0.202	–1.37
14.700	0.515	0.465	0.233	0.233	–10.78
17.140	0.480	0.442	0.320	0.320	–13.42
21.180	0.443	0.479	0.295	0.295	–11.14
25.260	0.318	0.372	0.443	0.443	–3.47
30.320	0.239	0.320	0.459	0.459	7.03
<i>T</i> = 513 K					
0.000	1.011	0.000	0.000	0.000	–
4.259	0.384	0.393	0.132	0.132	10.09
4.867	0.458	0.378	0.156	0.156	1.88
6.732	0.337	0.428	0.187	0.187	5.84
8.201	0.303	0.358	0.246	0.246	10.29
10.290	0.206	0.455	0.355	0.355	–4.45
19.890	0.106	0.331	0.560	0.560	1.38
24.830	0.033	0.148	0.836	0.836	–0.59
25.710	0.050	0.197	0.775	0.775	–1.09
<i>T</i> = 533 K					
0.000	1.010	0.000	0.000	0.000	–
0.900	0.799	0.222	0.078	0.078	–0.10
1.497	0.569	0.301	0.184	0.184	–4.36
1.921	0.390	0.317	0.327	0.327	–2.38
2.544	0.355	0.291	0.382	0.382	–1.78
2.668	0.266	0.294	0.481	0.481	–3.07
3.712	0.257	0.308	0.463	0.463	–1.78
4.832	0.108	0.267	0.687	0.687	–5.15
5.162	0.026	0.221	0.830	0.830	–6.63
8.230	0.009	0.105	0.982	0.982	–8.51
9.292	0.050	0.151	0.997	0.997	–18.60

hydrogenolysis can be represented by scheme (III), including the following steps:



$$\begin{aligned}
 w_1 &= k_1 P_A P_{H_2} [Z] - k_{-1} [ZAH_2], \\
 w_2 &= k_2 [ZAH_2], \\
 w_3 &= k_3 P_{H_2} [ZX], \\
 w_4 &= k_4 [ZB] - k_{-4} P_B [Z], \\
 w_5 &= k_5 P_B P_{H_2} [Z], \\
 w_6 &= k_6 [ZY] P_{H_2}, \\
 w_7 &= k_7 [ZCD] - k_{-7} [Z] P_C P_D.
 \end{aligned} \tag{III}$$

Steps (1)–(4) give overall reaction (I), and steps (5)–(7) give reaction (II).

When deriving equations, we assumed that the catalyst surface is uniform, the process occurs in the steady-state regime, and the balance of the surface coverage is fulfilled. By analogy with the conclusion made in [8–10], step (2) (dihydrothiophene formation) and step (5) (the formation of a surface complex of partially decomposed tetrahydrothiophene and hydrogen) are slow. Assuming equilibrium between the direct and reverse reactions in steps (1), (4), and (7), we determined the

[H_2], [ZB], and [ZCD] values. Setting the equality of the rates $w_1 = w_3 = w_6$, we calculated the [ZX] and [ZY] values. By substituting these values into the equation $[Z] + [ZAH_2] + [ZX] + [ZB] + [ZY] + [ZCD] = 1$, we obtained [Z]. By inserting this value into the equation for the rates of slow steps (2) and (5), we derived equations for the rates of thiophene hydrogenation (W_1) and tetrahydrothiophene decomposition (W_2) (henceforth, A is thiophene, B is tetrahydrothiophene, D is hydrogen sulfide, C is butane, and H_2 is hydrogen)

$$W_1 = \frac{k_2 (k_1/k_{-1}) y_A y_{H_2} P^2}{1 + \frac{k_1}{k_{-1}} y_A y_{H_2} P^2 + \left(\frac{k_1}{k_3} + \frac{k_1}{k_6}\right) y_A P + \frac{k_{-4}}{k_4} y_B P + \frac{k_{-7}}{k_7} y_D y_C P^2}, \tag{1}$$

$$W_2 = \frac{k_5 (k_1/k_{-1}) y_B y_{H_2} P^2}{1 + \frac{k_1}{k_{-1}} y_A y_{H_2} P^2 + \left(\frac{k_1}{k_3} + \frac{k_1}{k_6}\right) y_A P + \frac{k_{-4}}{k_4} y_B P + \frac{k_{-7}}{k_7} y_D y_C P^2}. \tag{2}$$

Determination of the Rate Constants of the Kinetic Model

The mathematical description of kinetic experiments carried out in a plug-flow reactor can be represented in the form of a system of the following differential equations

$$\frac{dy_A}{d\tau} = -W_1, \tag{3}$$

$$\frac{dy_B}{d\tau} = W_1 - W_2, \tag{4}$$

$$\frac{dy_D}{d\tau} = \frac{dy_C}{d\tau} = W_2, \tag{5}$$

$$\frac{dy_{H_2}}{d\tau} = -2(W_1 + W_2) \tag{6}$$

$$\text{at } \tau = 0: y_A = y_A^0; y_{H_2} = y_{H_2}^0; y_B = y_D = y_C = 0. \tag{7}$$

The problem is in determining the unknown constants in the equations for the rates W_1 and W_2 .

The parameters were estimated by an explicit integral method [11] with further analysis of the results by the method of scaling the main components [12]. Unfortunately, we failed to reliably estimate the constants in the denominator of rate equations (1) and (2). The experimental data were insensitive to these constants. Therefore, the overall equations for the rates can be reduced to the first-order equations with respect to the organic compounds. The molar fraction of hydrogen in the reaction mixture is very close to unity, and

the partial hydrogen pressure can be set equal to the total pressure in the system. Taking into account all these results, further identification of the model was performed using the following simplified empirical rate equations

$$W_1 \approx k_{1\text{app}} y_A, \quad W_2 \approx k_{2\text{app}} y_B, \quad (8)$$

where $k_{1\text{app}}$ and $k_{2\text{app}}$ are the apparent rate constants represented as functions of the temperature $\bar{k}(T)$ and the total pressure $F(P)$ in the system

$$k_{1\text{app}} = \bar{k}_1(T)F_1(P), \quad k_{2\text{app}} = \bar{k}_2(T)F_2(P). \quad (9)$$

Table 2 presents the $k_{1\text{app}}$ and $k_{2\text{app}}$ values ($\text{mmol g}^{-1} \text{s}^{-1}$) at $P = 2.06 \text{ MPa}$ at three temperatures. Table 2 shows that the estimates of the first-order rate constants are reliable, their confidence intervals being within 10% from the rate constant values.

Figure 1 compares the experimental and calculated data at three temperatures and $P = 2.06 \text{ MPa}$. Curves 1–3 show that simplified model (8) provides a good description of the experimental data at all studied temperatures.

Temperature Dependence of the Rate Constants

Figure 2 illustrates the temperature dependence of the apparent rate constants in the $\ln k_{i\text{app}}$ vs. $1000/T$ coordinates and suggests that the Arrhenius equation is satisfactorily described the effect of temperature on the reaction rates. The activation energies are $E_1 = 116 \text{ kJ/mol}$ and $E_2 = 132 \text{ kJ/mol}$ for reactions (I) and (II), respectively. Therefore, we took the first-order reactions and the Arrhenius dependence of the rate constants as a basis for further data processing.

Pressure Dependence of the Reaction Rates

To study the effect of the total pressure, we determined the apparent rate constants in an experimental series carried out at $T = 513 \text{ K}$ and pressures ranging from 0.2 to 3.0 MPa. Figure 3 illustrates the effect of pressure on the rate constants. The data of Fig. 3 are well approximated by exponential functions. Therefore, the functions in Eqs. (9) can be represented in the forms

$$F_1(P) \sim P^{n_1}, \quad F_2(P) \sim P^{n_2}. \quad (10)$$

The primary estimates of n_1 and n_2 , obtained using the least-square method with linearized forms

$$\ln k_{i\text{app}} = \ln a + n_i \ln P, \quad i = 1, 2 \quad (11)$$

are

$$n_1 = 0.5, \quad n_2 = 0.17. \quad (12)$$

Considering the above estimates for the activation energies and the exponents to be a good initial approximation, we performed the final statistical check of

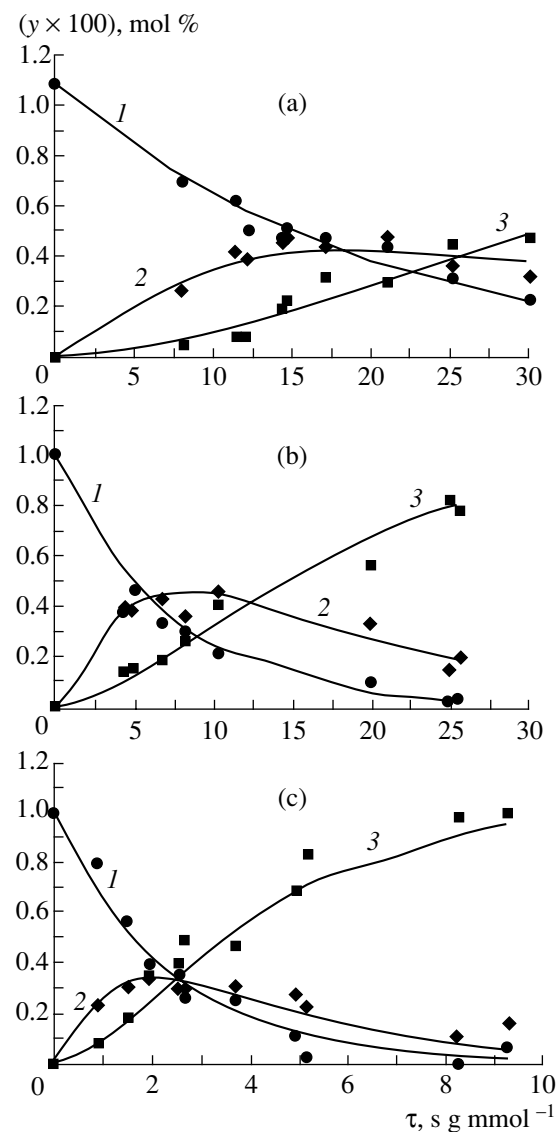


Fig. 1. Distribution of the reaction mixture component as a function of the contact time: (1) thiophene, (2) tetrahydrothiophene, and (3) hydrogen sulfide at $P = 2.06 \text{ MPa}$ and $T =$ (a) 493, (b) 513, and (c) 533 K. The points correspond to the experimental data and the lines represent the calculations according to the model.

model (3)–(7) using all experimental data obtained at temperatures of 493, 513, and 533 K and pressures equal to 0.21, 0.48, 0.99, 1.44, 2.06, and 3.07 MPa.

In this case, the rate equations are

$$W_1 = \bar{k}_{1,0} \exp\left(-\frac{E_1}{RT}\right) P^{n_1} y_A, \quad (13)$$

$$W_2 = \bar{k}_{2,0} \exp\left(-\frac{E_2}{RT}\right) P^{n_2} y_B. \quad (14)$$

Upon model identification, we determined the rate constants $\bar{k}_{1,0}$ and $\bar{k}_{2,0}$ and the more accurate values of E_1 ,

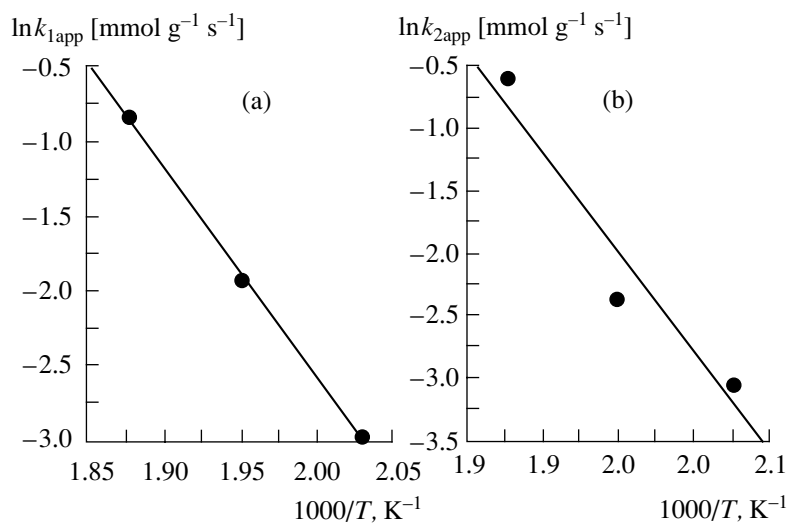


Fig. 2. Arrhenius plot of the apparent rate constants (a) $k_{1\text{app}}$ and (b) $k_{2\text{app}}$ at $P = 2.06$ MPa.

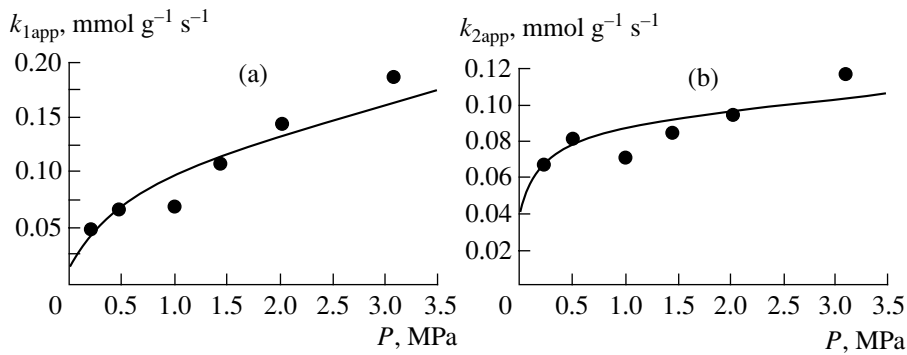


Fig. 3. Pressure dependence of the apparent rate constants (a) $k_{1\text{app}}$ and (b) $k_{2\text{app}}$ ($T = 513$ K).

E_2 , n_1 , and n_2 , as well as their confidence intervals. Table 3 summarizes the final identification results.

Statistical Data from All Experiments:

The number of the experimental data, 274;
The number of degrees of freedom, 268;
The t -criterion at a confidence probability of 95%, and 1.963;
The root-mean-square error the data description, 29%.

Table 2. Temperature dependence of the apparent rate constants. $P = 2.06$ MPa

T , K	$k_{1\text{app}}$, mmol g ⁻¹ s ⁻¹	$k_{2\text{app}}$, mmol g ⁻¹ s ⁻¹
493	0.05225 ± 0.00262	0.04836 ± 0.00485
513	0.14563 ± 0.01106	0.09539 ± 0.00934
533	0.43777 ± 0.01660	0.54861 ± 0.02226

Figure 4 compares the experimental and calculated data and shows that the model agrees well with the experimental data. A relatively great scatter of data for tetrahydrothiophene contributes significantly to the root-mean-square deviation of the experimental and calculated data. At the same time, Fig. 4 indicates that this scatter is random and independent of the systematic deviations of the experimental and calculated data. This supports the adequacy of the proposed kinetic model.

Table 3. Rate constants of the kinetic model

$\bar{k}_{1,0}$, mmol s ⁻¹ g ⁻¹ MPa ^{-0.495}	$6.9339 \times 10^{10} \pm 1.4388 \times 10^9$
$\bar{k}_{2,0}$, mmol s ⁻¹ g ⁻¹ MPa ^{-0.168}	$2.1677 \times 10^{12} \pm 8.7452 \times 10^{10}$
E_1 , kJ/mol	115.9 ± 5.1
E_2 , kJ/mol	131.8 ± 36.7
n_1	0.495 ± 0.202
n_2	0.168 ± 0.142

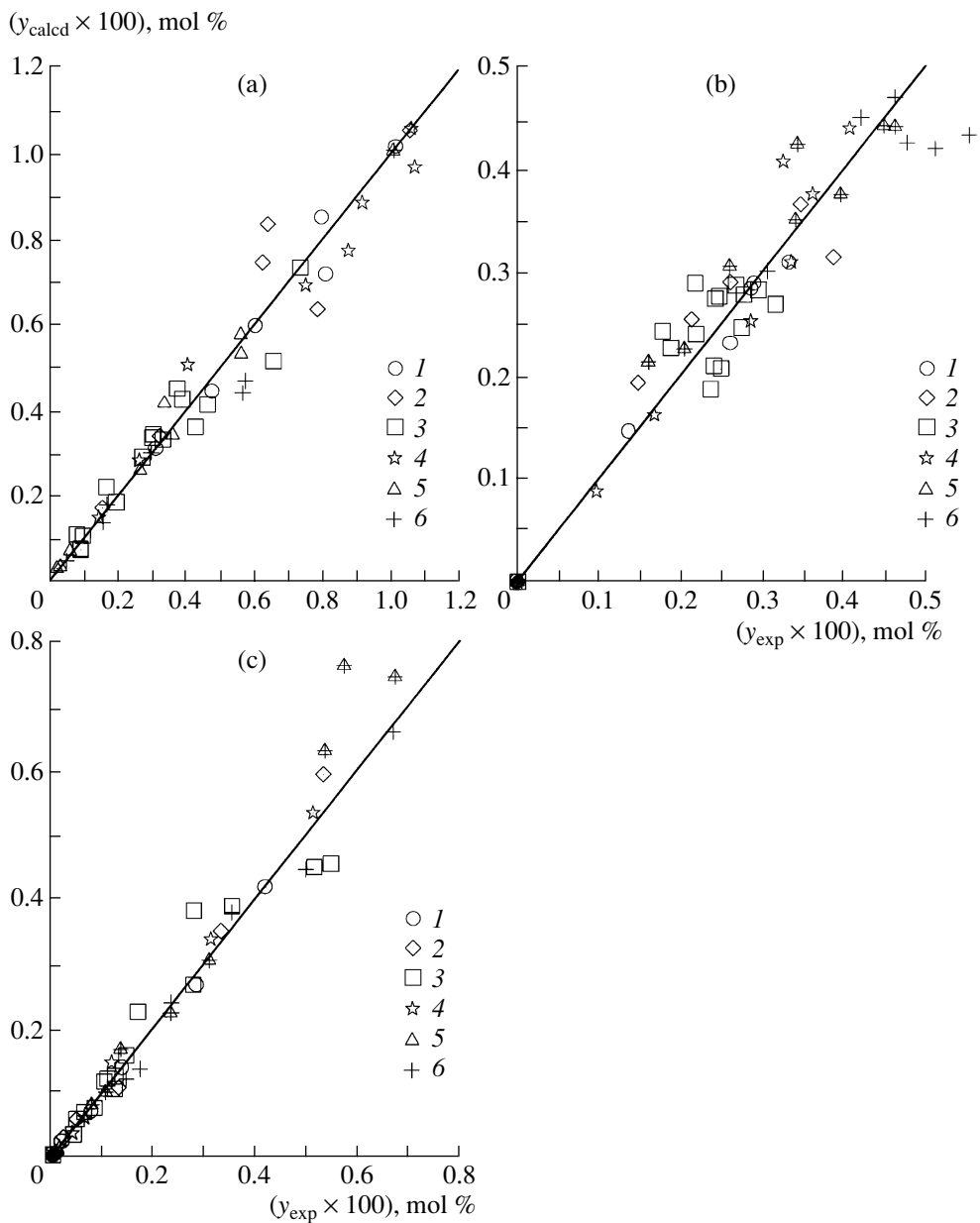


Fig. 4. Comparison of the experimental and calculated data obtained for (a) thiophene, (b) tetrahydrothiophene, and (c) H_2S at $T = 513 \text{ K}$ and $P, \text{ MPa}$: (1) 0.21, (2) 0.48, (3) 0.99, (4) 1.44, (5) 2.06, and (6) 3.07.

Selectivity to Tetrahydrothiophene

The differential selectivity to tetrahydrothiophene (S_{dif}) is expressed as a ratio of the rate of its accumulation to the rate of thiophene consumption (m_A is the number of thiophene moles, m_B is the number of the tetrahydrothiophene moles):

$$S_{\text{dif}}(\tau) \equiv \frac{dm_B}{-dm_A} = 1 - \frac{W_2}{W_1} \quad (15)$$

$$= 1 - \frac{k_{2,0}y_B(\tau)}{k_{1,0}y_A(\tau)} \exp(-(E_2 - E_1)/RT) P^{n_2 - n_1}.$$

Function (15) is equal to unity at $\tau = 0$ and tends to $-\infty$ at $y_A(\tau) \rightarrow 0$, that is, at $X = 1$ (where X is the conversion: $X = (y_A^0 - y(\tau))/y_A^0$). The selectivity decreases with an increase in temperature, because $E_2 > E_1$ and increases with an increase in pressure, since $n_2 - n_1 < 0$, $W_1 = W_2$, $S_{\text{dif}}(\tau) = 0$. At the maximum yield of the target product when $W_1 = W_2$, $S_{\text{dif}}(\tau) = 0$. Similarly, the integral selectivity S_{int} is equal to the ratio of the number of target product moles $m_B(\tau)$ to the number of moles of the reacted initial substance $m_A^0 X$ by time τ :

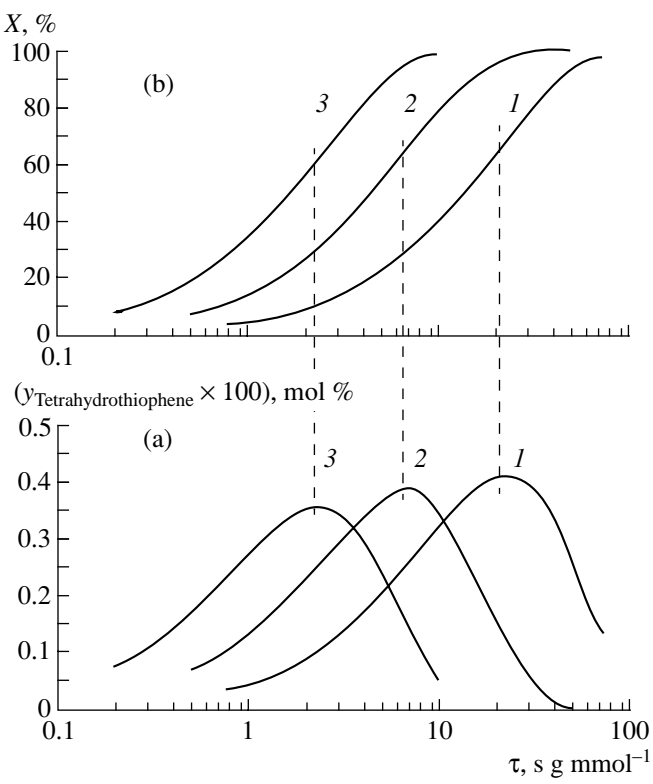


Fig. 5. (a) Tetrahydrothiophene yield and (b) conversion vs. contact time at (1) 493, (2) 513, and (3) 533 K. $P = 2.0$ MPa.

$$S_{\text{int}}(\tau) \equiv \frac{m_B}{m_A X} = \frac{y_B(\tau)}{y_A^0 X(\tau)} = \frac{y_B(\tau)}{y_A^0 - y_A(\tau)}, \quad (16)$$

$$y_B(\tau) = \int_0^\tau (W_1(\tau) - W_2(\tau)) d\tau, \quad (17)$$

$$y_A^0 - y_A(\tau) = \int_0^\tau W_1(\tau) d\tau.$$

$$\varphi(\tau) \equiv 1 - \frac{k_{2\text{app}}}{k_{2\text{app}} - k_{1\text{app}}} \frac{1}{y_A^0} [1 - \exp(-(k_{2\text{app}} - k_{1\text{app}})\tau)] = 0. \quad (24)$$

By substituting the solution to Eq. (24) into Eqs. (20) and (21), one can determine the values of $y_B^*(\tau^*)$ and $X^*(\tau^*)$. The influence of temperature and pressure on these parameters is determined by Eqs. (22) and (23).

Figure 5 illustrates the graphical solution to the problem as plots of conversion and the tetrahydrothiophene yield vs. the contact time at 493, 513, and 533 K and 2.0 MPa. Figure 5 shows that, with an increase in temperature, the maximum yield of tetrahydrothiophene decreases from 0.4 to 0.35% and the con-

version, corresponding to the maximum, decreases insignificantly. The contact time τ necessary for the attainment of the maximum tetrahydrothiophene yield increases by a factor of ~10 as the temperature decreases by 40 K. From this standpoint, the low-temperature process is not the optimal one, despite the high tetrahydrothiophene yield.

When determining the best operating conditions, the parameters governing the maximal yield of the target product $y_B^*(\tau^*)$ are the most illustrative

$$\frac{dy_B}{d\tau} = W_1 - W_2 = 0. \quad (18)$$

From condition (18), one can determine the coordinates of the maximum: the contact time τ^* and the conversion $X^*(\tau^*)$ at a maximum point. Generally, these parameters depend on the type of the rate equations and the rate constants and are determined directly by the numerical integration of the differential rate equations.

Taking into account the first reaction order, functions $y_B(\tau)$ and $X(\tau)$ can be obtained in the analytical form:

$$y_A(\tau) = y_A^0 \exp(-k_1 \tau), \quad (19)$$

$$y_B(\tau) = \frac{k_{1\text{app}}}{k_{2\text{app}} - k_{1\text{app}}} y_A^0 [\exp(-k_{1\text{app}}\tau) - \exp(-k_{2\text{app}}\tau)] \quad (20)$$

at $y_B^0 = 0$,

$$X(\tau) = 1 - \exp(-k_{1\text{app}}\tau), \quad (21)$$

where $k_{1\text{app}}$ and $k_{2\text{app}}$ are the rate constants expressed according to Eqs. (13) and (14) as

$$k_{1\text{app}} = \bar{k}_{1,0} \exp\left(-\frac{E_1}{RT}\right) P^{n_1}, \quad (22)$$

$$k_{2\text{app}} = \bar{k}_{2,0} \exp\left(-\frac{E_2}{RT}\right) P^{n_2}. \quad (23)$$

The contact time τ^* corresponding to condition (18), that is, to the maximum yield of the target product, is the solution to the nonlinear equation

version, corresponding to the maximum, decreases insignificantly. The contact time τ necessary for the attainment of the maximum tetrahydrothiophene yield increases by a factor of ~10 as the temperature decreases by 40 K. From this standpoint, the low-temperature process is not the optimal one, despite the high tetrahydrothiophene yield.

Figure 6 illustrates how the contact time influences the tetrahydrothiophene yield and the conversion at 1.0, 2.0, and 3.0 MPa and 513 K and shows that the y_B^*

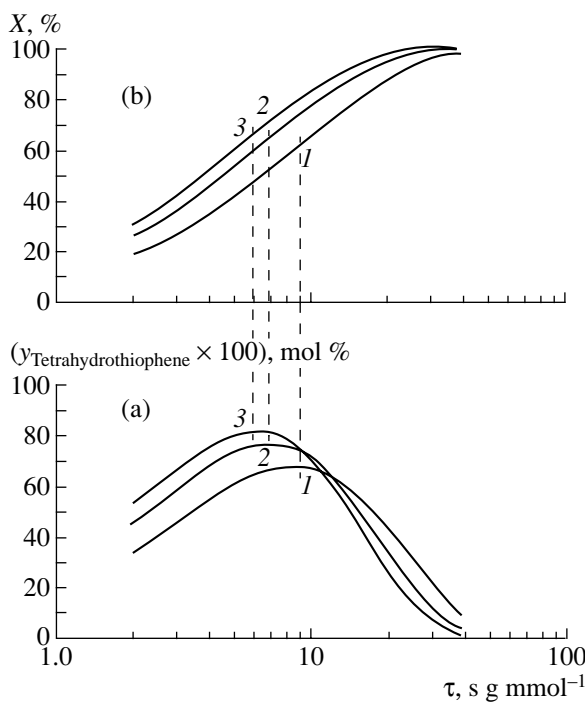


Fig. 6. (a) Tetrahydrothiophene yield and (b) conversion vs. contact time at pressures of (1) 1.0, (2) 2.0, and (3) 3.0 MPa. $T = 513$ K.

value increases with pressure. This is accompanied by changes in the parameters corresponding to the coordinates of the maximum: the contact time τ^* shortens, and the conversion X^* increases. Therefore, the total pressure in the system is a more efficient factor governing the process than the temperature.

REFERENCES

1. Mashkina, A.V., *Geterogennyi kataliz v khimii organicheskikh soedinenii sery* (Heterogeneous Catalysis in the Chemistry of Organosulfur Compounds), Novosibirsk: Nauka, 1977.
2. Obolentsev, R.D. and Mashkina, A.V., *Gidrogenoliza seraorganicheskikh soedinenii nefti* (Hydrogenolysis of Organosulfur Compounds of Oil), Moscow: Gostoptekhizdat, 1961.
3. Mashkina, A.V., *Sulfur Rep.*, 1991, vol. 10, no. 4, p. 279.
4. Ermakova, A., Anikeev, V.I., and Froment, J.F., *Teor. Osn. Khim. Tekhnol.*, 2000, vol. 34, no. 2, p. 203.
5. Ermakova, A., *Metody makrokinetiki, primenyaemye pri matematicheskem modelirovani khimicheskikh protsessov i reaktorov* (Methods of Macrokinetics in the Mathematical Modeling of Chemical Reactors), Novosibirsk: Inst. of Catal., 2001.
6. Mashkina, A.V. and Sakhaltueva, L.G., *Kinet. Katal.*, 2002, vol. 43, no. 1, p. 116.
7. Saur, N.N., Markel, E.J., Schrader, G.I., and Angelici, R.J., *J. Catal.*, 1989, vol. 117, no. 1, p. 295.
8. Navalikhina, M.D. and Krylova, O.V., *Usp. Khim.*, 1998, vol. 67, no. 7, p. 656.
9. Temkin, M.I., Murzin, D.Yu., and Kul'kova, N.V., *Kinet. Katal.*, 1989, vol. 30, no. 3, p. 637.
10. Van Meerten, R.Z.C. and Coenen, W.E., *J. Catal.*, 1977, vol. 46, no. 1, pp. 13–24.
11. Yermakova, A., Valko, P., and Vajda, S., *Appl. Catal.*, 1982, vol. 2, no. 3, p. 139.
12. Ermakova, A., *Matematicheskoe modelirovani kataliticheskikh reaktorov* (Mathematical Modeling of Chemical Reactors), Matros, Yu. Sh., Ed., 1989, p. 120.